

# Magnetic-field induced band-structure change in CeBiPt

N. Kozlova<sup>1</sup>, J. Hagel<sup>2</sup>, M. Doerr<sup>2</sup>, J. Wosnitza<sup>2[\*]</sup>, D. Eckert<sup>1</sup>, K.-H. Müller<sup>1</sup>, L. Schultz<sup>1</sup>, I. Opahle<sup>1</sup>, S. Elgazzar<sup>1</sup>, Manuel Richter<sup>1</sup>, G. Goll<sup>3</sup>, H. v. Löhneysen<sup>3,4</sup>, G. Zwicknagl<sup>5</sup>, T. Yoshino<sup>6</sup>, T. Takabatake<sup>6</sup>

<sup>1</sup>*Institut für Festkörper- und Werkstofforschung (IFW) Dresden, D-01171 Dresden, Germany*

<sup>2</sup>*Institut für Festkörperphysik, Technische Universität Dresden, D-01062 Dresden, Germany*

<sup>3</sup>*Physikalisches Institut, Universität Karlsruhe, D-76128 Karlsruhe, Germany*

<sup>4</sup>*Forschungszentrum Karlsruhe, Institut für Festkörperphysik, D-76021 Karlsruhe, Germany*

<sup>5</sup>*Institut für Mathematische Physik, Technische Universität Braunschweig, D-38106 Braunschweig, Germany*

<sup>6</sup>*Department of Quantum Matter, ADSM, Hiroshima University, Higashi-Hiroshima 739-8530, Japan*

(Dated: March 23, 2022)

We report on a field-induced change of the electronic band structure of CeBiPt as evidenced by electrical-transport measurements in pulsed magnetic fields. Above  $\sim 25$  T, the charge-carrier concentration increases nearly 30% with a concomitant disappearance of the Shubnikov-de Haas signal. These features are intimately related to the Ce  $4f$  electrons since for the non- $4f$  compound LaBiPt the Fermi surface remains unaffected. Electronic band-structure calculations point to a  $4f$ -polarization-induced change of the Fermi-surface topology.

PACS numbers: 71.18.+y, 71.20.Eh, 72.15.Gd

The influence of magnetic fields on the electronic band structure of metals is usually minute and may, therefore, in most cases be disregarded because of the different relevant energy scales of the itinerant electrons in conventional metals and of the applied magnetic fields: the typical Fermi energy is of the order eV compared to a Zeeman energy of  $\sim 6$  meV at 50 T. However, the situation may change considerably in case the relevant energy scales of the electronic system are strongly reduced.

Prominent examples for field-induced changes of the Fermi surface are, e.g., strongly correlated metals close to a “quantum critical point” [1]. Usually, the criticality results from magnetic interactions leading to field-induced modifications of the magnetic ground state [2, 3]. For some materials different Fermi surfaces could be detected above and below a metamagnetic phase transition [2, 4, 5]. In the paramagnetic state of a metal, however, a direct influence of an external magnetic field on the electronic band structure is usually not expected.

Here, we provide evidence for a rather sudden field-induced increase of the charge-carrier concentration connected with a Fermi-surface change in the semimetal CeBiPt. This remarkable phenomenon is absent in the non- $4f$  sister compound LaBiPt. Both compounds belong to the intermetallic series  $R\text{BiPt}$  ( $R$  = rare-earth metal) that shows a rich diversity of ground states depending on  $R$  [6]. Explicitly, YbBiPt is a “super”-heavy-fermion metal [7], NdBiPt is a small-gap semiconductor [6], LaBiPt is a superconductor with critical temperature  $T_c = 0.9$  K, and CeBiPt is a commensurate antiferromagnet with an ordering temperature of  $T_N = 1.1$  K [8, 9].

In the following we present high-field investigations of the magnetization and of the electrical-transport properties of LaBiPt and CeBiPt in the paramagnetic metallic state. Both compounds are semimetals with very low charge-carrier concentrations and correspondingly

small Fermi surfaces [9]. The electronic properties of LaBiPt can consistently be described by standard Fermi-liquid theory. The observed magnetic quantum oscillations [9, 10] agree very well with band-structure calculations [11]. The picture changes considerably for the isostructural semimetal CeBiPt. Above  $\sim 10$  K and below  $\sim 20$  T, the electronic properties follow conventional Fermi-liquid theory as in LaBiPt. Towards lower temperatures, however, the Fermi surface changes, i.e., for certain field orientations the Shubnikov-de Haas (SdH) frequency increases by almost a factor of two between 10 and 0.4 K [9]. Another unusual feature is found in pulsed-field experiments. Above about 25 T the SdH signal vanishes and, instead, the magnetoresistance increases considerably (Fig. 1) hinting at a field-induced Fermi-surface modification [10]. This feature is not related to the quantum limit since at 25 T still about five Landau levels (of both spin orientations) are occupied.

The single crystals of CeBiPt and LaBiPt were grown at Hiroshima University by use of the Bridgman technique. Details of the crystal growth have been reported elsewhere [8, 9]. The electrical-transport and magnetization measurements were performed at the High Magnetic Field Laboratory Dresden (HLD) in pulsed fields up to about 50 T at temperatures above  $T = 1.8$  K by use of a  $^4\text{He}$  gas-flow cryostat. For the transport measurements six  $40\text{ }\mu\text{m}$  gold wires were attached to the samples with graphite paste. AC currents up to 1 mA with frequencies between 10 and 50 kHz were applied for about 80 ms just before and during the field pulse. The reliability of the data was checked for different currents and frequencies. Uncertainties of the geometry factors result in error bars of about 20% in the absolute resistivity. The samples were tightly fixed to the sample holder with IMI7031 varnish. Since small misalignments of the contacts are unavoidable the longitudinal and transverse

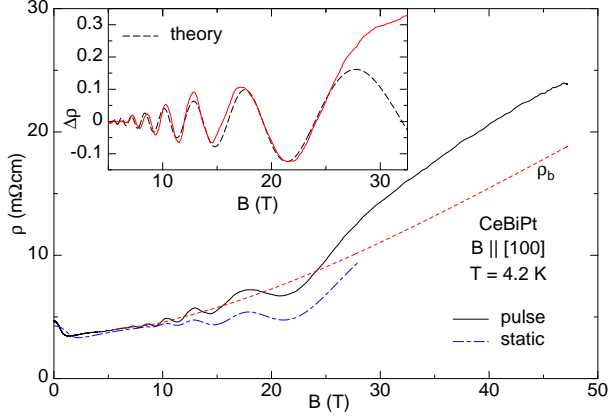


FIG. 1: Field dependence of the resistivity of CeBiPt at 4.2 K in a pulsed field of up to 48 T and in a static field of up to 28 T. The inset shows the SdH signal after subtracting the steady background  $\rho_b$  from the pulsed-field data. The dashed curve represents the behavior expected theoretically.

(Hall) resistances were extracted from positive and negative field pulses applied successively at each temperature [12]. The data shown in the following, therefore, comprise either the completely symmetric (longitudinal) and antisymmetric (transverse) signals.

The overall agreement between pulsed-field and static-field data is very good (Fig. 1) [9]. The initial decrease of the resistivity,  $\rho$ , reflects most probably antiferromagnetic fluctuations above  $T_N$  in the paramagnetic state as evident from its absence at 20 K [10]. Then, up to about 25 T, the oscillations caused by the SdH effect appear. Towards higher fields, however, instead of exhibiting further maxima and minima,  $\rho$  just increases monotonically.

The inset in Fig 1 shows the expected SdH signal (dashed curve) in comparison to the experimental data. For the theory curve we used the well-known SdH formulas (see [13] for details) with parameters  $F = 48$  T for the SdH frequency,  $m_c = 0.24 m_e$  for the effective mass, and  $T_D = 2.7$  K for the Dingle temperature, in good agreement with the static-field data [9]. For the experimental signal we plotted  $\Delta\rho = (\rho - \rho_b)/\rho_b$ , with  $\rho_b$  the steady background resistivity shown by the dashed line in Fig. 1 [14]. It is evident that above 25 T the oscillating signal disappears. We should note that there is some ambiguity determining  $\rho_b$ . However, in order to recover an oscillating behavior of  $\Delta\rho$  above 25 T a highly artificial oscillatory background would have to be assumed.

In previous experiments, it was shown that the resistance increase can be followed up to 60 T and that the SdH oscillations vanish independent of sample orientation in field [10]. This contrasts with the temperature-dependent change of the Fermi surface that occurs only for fields aligned within about 15 deg along the main cubic-lattice axes [9].

In order to investigate the high-field behavior of Ce-

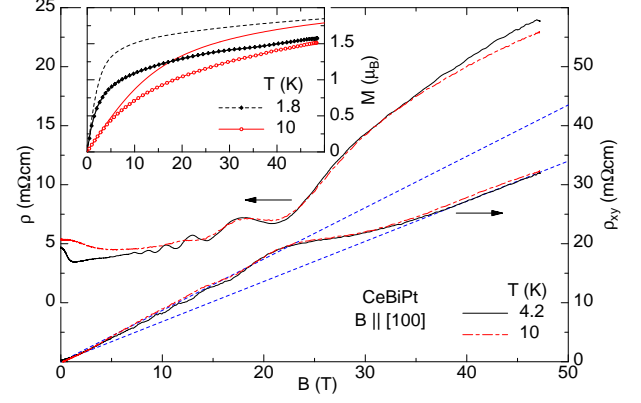


FIG. 2: Field dependence of the longitudinal and transverse resistivities of CeBiPt for different temperatures. The dashed lines are linear fits to the low and high-field Hall data. The inset shows the measured (symbols) in comparison to the calculated magnetization (lines).

BiPt in more detail, we measured the Hall effect. Indeed, as the most important result of this study, Hall-effect measurements in pulsed fields reveal a clear change of slope of the Hall signal at this field range (Fig. 2). This effect was found to be temperature independent between 1.8 and 10 K. Matching the field where the strong increase of the longitudinal resistance sets in, the average Hall coefficient,  $R_H = \rho_{xy}/B$ , decreases by about 28% (difference in the slopes of the two dashed lines in Fig. 2). The fit to the low-field ( $B \lesssim 22$  T) Hall data results in a hole-like charge-carrier concentration of  $n_h^{low} = (R_H e)^{-1} = 7.2(3) \times 10^{17} \text{ cm}^{-3}$ , whereas at high fields ( $B \gtrsim 38$  T) it increases to  $n_h^{high} = 9.2(3) \times 10^{17} \text{ cm}^{-3}$ . The low-field value agrees well with the result of static-field measurements ( $n_h^{low} = 7.7 \times 10^{17} \text{ cm}^{-3}$  [9]) in view of the experimental error caused mainly by the sample-geometry uncertainties.

It is this field-induced increase of the charge-carrier concentration that is unique for the present paramagnetic metal. Earlier band-structure calculations resulted in two small hole-like Fermi surfaces at the Brillouin-zone center and even smaller electron-like Fermi surfaces surrounding them [9]. Assuming a simple single-band picture, the low-field (below 25 T) SdH results are in line with these calculations, although the smallness of the electron pockets prohibits an experimental verification by our SdH measurements. From theory it is not clear how this band structure is modified above 25 T. A detailed analysis of the high-field Fermi-surface topology from our data is excluded due to the lack of any detectable SdH signal at these fields. The increasing number of hole-like charge carriers would lead to a small increase (by about 18%) of the SdH frequency.

The temperature-dependent Fermi-surface change was found only for CeBiPt, but not for the homologous non-

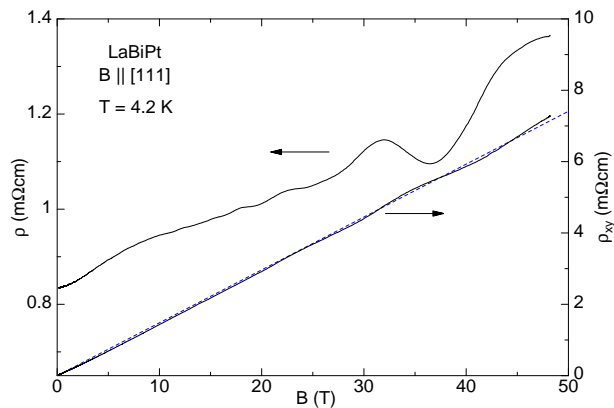


FIG. 3: Field dependence of the longitudinal and transverse resistivities of LaBiPt. The dashed line is a linear fit to the Hall data.

4*f* compound LaBiPt [9]. It was, therefore, straightforward to check for any unusual field-induced phenomena in LaBiPt. As shown in Fig. 3, for this metal neither the longitudinal resistance nor the Hall effect reveal any deviation from a well-behaved Fermi liquid. The SdH signal for LaBiPt can be well explained [10] by two slightly different hole-like Fermi surfaces as predicted by band-structure calculations [11]. Most notably, the transverse signal increases – except for small SdH traces – linearly with magnetic field without any unusual slope change. Consequently, the charge-carrier concentration in LaBiPt remains at  $n_h = 4.2(2) \times 10^{18} \text{ cm}^{-3}$  independent of field.

These results clearly show that the Ce 4*f* electrons are responsible for the observed field-induced band-structure modifications. A partial onset of 4*f* hybridization was suggested to explain the temperature-dependent change of the Fermi-surface area observed earlier [9]. Thus, one possible scenario for the observed feature would be that with increasing magnetic field the *f* electrons become decoupled from the delocalized electrons. This may lead to a reduced number of electron-like states which in turn would result in an increased value  $n_h^{\text{high}}$  for the hole-like charge-carrier concentration. A field-dependent decrease of the 4*f* hybridization is well known from Ce-based heavy-fermion compounds, such as CeCu<sub>6</sub> and CeB<sub>6</sub> [15]. It should be noted, however, that in contrast to these materials the Kondo effect appears to play no significant role in CeBiPt. The Sommerfeld coefficient  $\gamma$  deduced from specific-heat measurements is very low [8] and the effective mass from SdH measurements is only 0.24 free-electron masses [9]. We further observe a rather sudden change of the charge-carrier concentration in CeBiPt that contrasts the smooth effective-mass decrease in the above heavy-fermion systems.

As a consequence of the *f* electrons losing their itinerant character one would expect a structure in the magnetization,  $M$ , with increasing field, i.e., some increase

of  $M$  at about 25 T. We, thus, measured  $M$  of a large (374.5 mg) CeBiPt single crystal in pulsed magnetic fields up to about 49 T. As shown in the inset of Fig. 2, there is no significant feature visible at 25 T in the magnetization  $M(B)$ . We therefore exclude a field-induced decoupling of the *f* electrons from the itinerant charge carriers.

The expected magnetization curves at 1.8 and 10 K (lines in the inset of Fig. 2) have been calculated assuming localized Ce 4*f* moments. All necessary information for this calculation is known; from inelastic neutron-scattering experiments of CeBiPt powder a crystal-electric-field (CEF) splitting of 9.5 meV has been measured [16] and specific-heat data show that the quartet  $\Gamma_8$  state has the lowest energy [8, 17]. Since the  $\Gamma_7$  doublet is well separated from  $\Gamma_8$  the free-ion saturation magnetization of  $2.14 \mu_B$  cannot be reached up to 50 T. The experimental data clearly fall below the expected  $M$ .

As an alternative scenario, the external field dependence of the band structure was checked. Though the Fermi surfaces are tiny, the direct Zeeman splitting of the band states is probably too small to explain the effect. Field-induced 4*f* polarization, however, produces an exchange field on the Ce 5*d* states that may yield band splittings of  $\sim 0.1$  eV at 50 T in the saturated state.

At first, the zero-field band structure of CeBiPt was re-calculated by use of a recent [18], high-precision four-component relativistic version of the full-potential local-orbital (FPLO) code [19]. The Perdew–Zunger parametrization of the exchange-correlation potential in the local spin-density approximation (LSDA) was used. A basis set of optimized local orbitals with 5*s*, 5*p*, 6*s*, 6*p*, and 5*d* states for Ce, Bi, and Pt was used. The Ce 4*f* electron was not included in the valence basis and localized by use of a confining potential. A spherically averaged 4*f* charge and spin density was assumed. Self-consistent calculations were performed with 8000 *k*-points in the full Brillouin zone and 2000 Fourier components per atom for the Ewald-potential representation. The effect of all technical details of the calculation (4*f* confinement, spherical 4*f* charge density, other numerical parameters) has been carefully checked to be below 10 meV in the region close to  $E_F$ .

The resulting band structure [Fig. 4(a)] is very similar to that published earlier [9], but the semi-metallic character is yet more prominent with almost vanishing Fermi surfaces. The experimentally observed hole-pocket areas can be matched if the Fermi level is shifted by 20 meV to lower energy. This shift corresponds to a tiny change of the valence electron number,  $\Delta N/N \approx 10^{-5}$ . Such an uncertainty can be related either to a minute off-stoichiometry of the samples below the limit of detectability or to the limited accuracy of the LSDA used to calculate the single-electron levels.

Next, we note that all states in the vicinity of the Fermi level ( $\pm 0.5$  eV) have predominantly Ce-5*d* character. If 4*f* polarization is applied (using the so-called

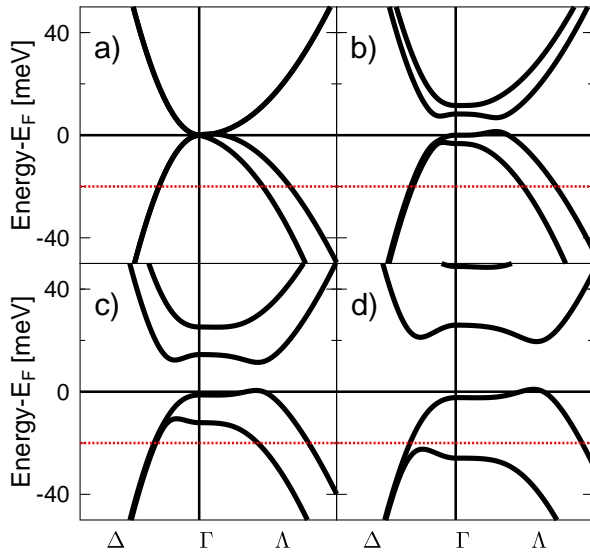


FIG. 4: LSDA bands of CeBiPt close to the Brillouin-zone center along the symmetry lines  $\Delta$  [from (0.100) to (000) in units of  $2\pi/a$ ] and  $\Lambda$  [from (000) to (0.067 0.067 0.067)]. The nominal  $E_F$  is at zero energy, the shifted Fermi level that yields the correct Fermi-surface area is indicated at  $-20$  meV by the dotted line. (a) shows the non-magnetic case with unpolarized  $4f$  shell; In (b), (c), and (d), the  $4f$  spin moment is fixed to be  $0.2\mu_B$ ,  $0.5\mu_B$ , and  $1.0\mu_B$ , respectively.

open-core approach), intra-atomic exchange interaction splits the Ce- $5d$  bands close to the center of the Brillouin zone [Fig. 4(b-d)]. The nominal Fermi level (integer number of valence electrons) is taken as reference (0 eV) and a shifted Fermi level that provides the correct Fermi-surface area is indicated by the dotted line. The  $4f$  spin polarization is gradually enhanced from compensated spin densities [Fig. 4(a)] to completely polarized  $4f$  state [Fig. 4(d)]. The latter situation corresponds to a field-saturated paramagnet. With increasing  $4f$  polarization, the electronic bands close to the Brillouin-zone center are split in a Zeeman-like fashion into four equidistant levels. Their splitting increases linearly with the  $4f$  spin moment up to  $\sim 75$  meV. The lowest of the four levels crosses the shifted Fermi level before the  $4f$  moment is saturated. The related change of the Fermi-surface topology could explain the measured Hall-effect peculiarity. It should be noted that this scenario, though being attractive by its simplicity, does not explain the observed temperature independence of the effect.

Conduction-electron scattering off virtual CEF excitations provides an alternative qualitative explanation. These processes enhance the effective masses and shift the conduction-electron energies. The shifts, being negligible in conventional metals, can affect the Fermi surfaces in semimetals with low carrier concentrations. The resulting field-induced changes should vary rather weakly with temperature as will be discussed elsewhere.

In conclusion, we have presented evidence for a dras-

tic change of the electronic band structure of CeBiPt at  $\sim 25$  T. Above this field the SdH oscillations vanish and the hole-like charge-carrier concentration increases by about 28%. The absence of these features in LaBiPt clearly reflects the relevance of the  $4f$  electrons for the observed behavior. A splitting of the Ce- $5d$  bands close to  $E_F$  due to exchange interaction with the polarized  $4f$  states is a possible explanation. This mechanism would yield a magnetic-field driven metal-insulator transition for exact stoichiometry.

We would like to thank O. Stockert, M. Rotter, and A. Möbius for inspiring discussions. The work at Dresden was supported by the DFG through SFB 463 and the BMBF (FKZ 035C5 DRE). The work at Hiroshima was supported by a grant for the International Joint Research Project NEDO and the COE Research (13E2002) in a Grant-in-Aid from the Ministry of Education, Culture, Sports, Science, and Technology of Japan. The work at Karlsruhe was supported by the DFG through SFB 195.

- 
- [\*] present address: Forschungszentrum Rossendorf, Hochfeld-Magnetlabor Dresden, 01314 Dresden, Germany
  - [1] S. Sachdev, *Quantum Phase Transitions* (Cambridge University Press, Cambridge, 1999).
  - [2] R. A. Borzi *et al.*, Phys. Rev. Lett. **92**, 216403 (2004) and references therein.
  - [3] K. H. Kim *et al.*, Phys. Rev. Lett. **91**, 256401 (2003); J. Custers *et al.*, Nature **424**, 524 (2003).
  - [4] S. R. Julian *et al.*, Physica B **199**, 63 (1994).
  - [5] H. Aoki *et al.*, Phys. Rev. Lett. **71**, 2110 (1993).
  - [6] P. C. Canfield *et al.*, J. Appl. Phys. **70**, 5800 (1991).
  - [7] Z. Fisk *et al.*, Phys. Rev. Lett. **67**, 3310 (1991).
  - [8] T. Pietrus *et al.*, Physica B **281-282**, 745 (2000).
  - [9] G. Goll *et al.*, Europhys. Lett. **57**, 233 (2002).
  - [10] J. Wosnitza *et al.*, Physica B **346-347**, 127 (2004).
  - [11] T. Oguchi, Phys. Rev. B **63**, 125115 (2001).
  - [12] For CeBiPt, due to technical reasons, the maximum negative field was limited to  $-17$  T. Anyway, a reliable disentangling of the longitudinal and transverse transport contributions was still possible.
  - [13] D. Shoenberg, *Magnetic Oscillations in Metals* (Cambridge University Press, Cambridge 1984).
  - [14] The correct SdH signal, i.e., the relative conductivity,  $\Delta\sigma/\sigma$ , results in the same physical conclusions.
  - [15] Z. Fisk and J.D. Thompson, in *Physical Phenomena at High Magnetic Fields*, edited by E. Manousakis *et al.* (Addison-Wesley, Redwood City, CA, 1992), p. 197 and references therein.
  - [16] O. Stockert and G. Goll, unpublished.
  - [17] R. Lortz *et al.*, unpublished.
  - [18] I. Opahle, PhD thesis, TU Dresden 2001; H. Eschrig, M. Richter, and I. Opahle, in: *Relativistic Electronic Structure Theory - Part II: Applications*, Ed. P. Schwerdtfeger (Elsevier, Amsterdam 2004) pp. 723–776.
  - [19] K. Koepf and H. Eschrig, Phys. Rev. B **59**, 1743 (1999); <http://www.FPLO.de>.